

SUPPLEMENTARY INFORMATION

Computational Insights into the pH-Dependent Behavior of Ipilimumab-CTLA-4

Wanda Destiarani^a, Kowit Hengphasatporn^b, Yasuteru Shigeta^b, and Ryuhei Harada^{*b}

^a Doctoral Program in Biology, University of Tsukuba, Tsukuba, Ibaraki 305-8572, Japan

^b Center for Computational Sciences, University of Tsukuba, Tsukuba, Ibaraki 305-8577, Japan

*Corresponding Author: ryuhei@ccs.tsukuba.ac.jp

Table S1. The protonation state assigned to each mutated residue in the light and heavy chains of all Ipilimumab variants for their molecular dynamics (MD) simulations using PROPKA3. Each residue name corresponds to the Amber format.

Variant	Residue	pKa Calculation using PROPKA3	Partial Protonation (pH 6.0)		Full Protonation (pH 4.5)	
			Physiological	Acidic	Physiological	Acidic
Ipi95	HIS 31	7.17	HID	HIP	HID	HIP
	HIS 56	6.70	HID	HIP	HID	HIP
	THR 99	–	THR	THR	THR	THR
	GLU 28	3.46	GLU	GLU	GLU	GLH
	ASP 31	3.86	ASP	ASP	ASP	ASH
	GLU 33	4.73	GLU	GLU	GLU	GLH
Ipi105	HIS 31	6.27	HID	HIP	HID	HIP
	HIS 56	6.92	HID	HIP	HID	HIP
	THR 99	–	THR	THR	THR	THR
	GLU 28	3.36	GLU	GLU	GLU	GLH
	GLU 31	4.77	GLU	GLU	GLU	GLH
	GLU 33	5.17	GLU	GLU	GLU	GLH
Ipi106	HIS 31	7.08	HID	HIP	HID	HIP
	HIS 56	7.08	HID	HIP	HID	HIP
	HIS 99	4.34	HID	HIP	HID	HIP
	GLU 28	3.32	GLU	GLU	GLU	GLH
	GLU 31	4.66	GLU	GLU	GLU	GLH
	GLU 33	4.59	GLU	GLU	GLU	GLH

Figure S1. Surface potentials of the antigen–antibody interfaces in all variants (Ipi95, Ipi105, Ipi106) under physiological and acidic conditions, comparing their partial and full protonation states. The surface potentials were calculated using the APBS program in PDB2PQR webserver,¹ and visualized using Biovia Discovery Studio 2024.²

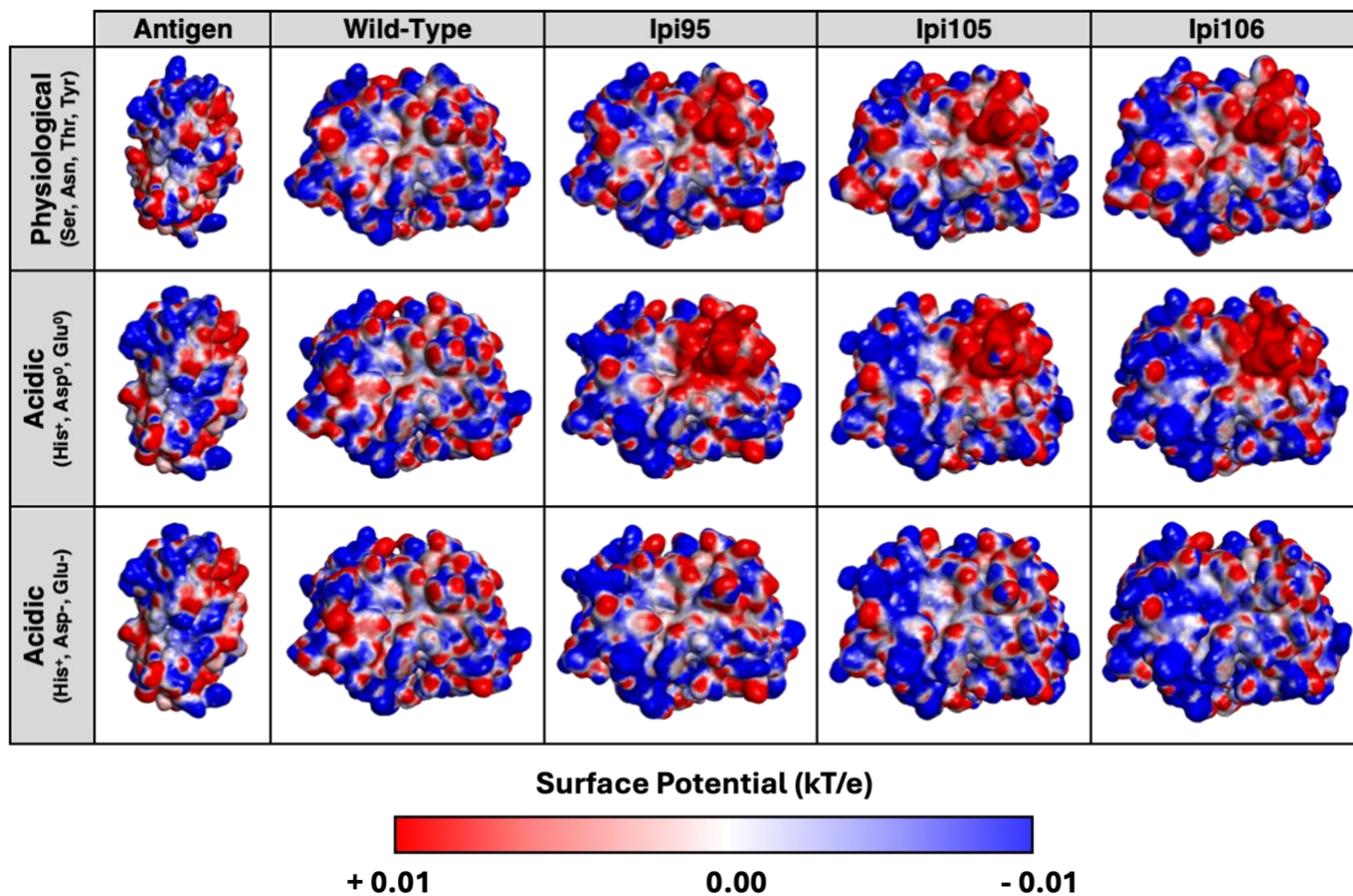


Table S2. The average MM/GBSA-based binding energy values of Ipilimumab–CTLA-4 complex binding in physiological and acidic conditions.

Variant	$\Delta G_{\text{MM/GBSA}}^* \pm \text{SE (kcal}\cdot\text{mol}^{-1})$		
	Physiological	Acidic	
	pH 7.4	pH 6.0	pH 4.5
Wild-Type	-12.9525 ± 1.71	-16.9126 ± 0.99	-16.9126 ± 0.99
Ipi95	-12.2721 ± 1.21	-16.8602 ± 1.14	-20.2615 ± 1.73
Ipi105	-10.2512 ± 2.35	-17.9574 ± 1.00	-19.5213 ± 2.78
Ipi106	-12.4499 ± 2.46	-18.8817 ± 3.19	-19.6413 ± 1.35

Figure S2. (A) Profiles of root-mean-square deviation (RMSD) and (B) root-mean-square fluctuation (RMSF) for the antigen–antibody complexes, calculated using over five 500-ns MD replicas.⁵ Blue and red lines represent the physiological and acidic conditions, respectively; bold lines show mean values, while lighter lines indicate individual replicas. Profiles of RMSF were compared with the Wild-Type. Graphs were generated using ggplot² in JupyterLab.⁴

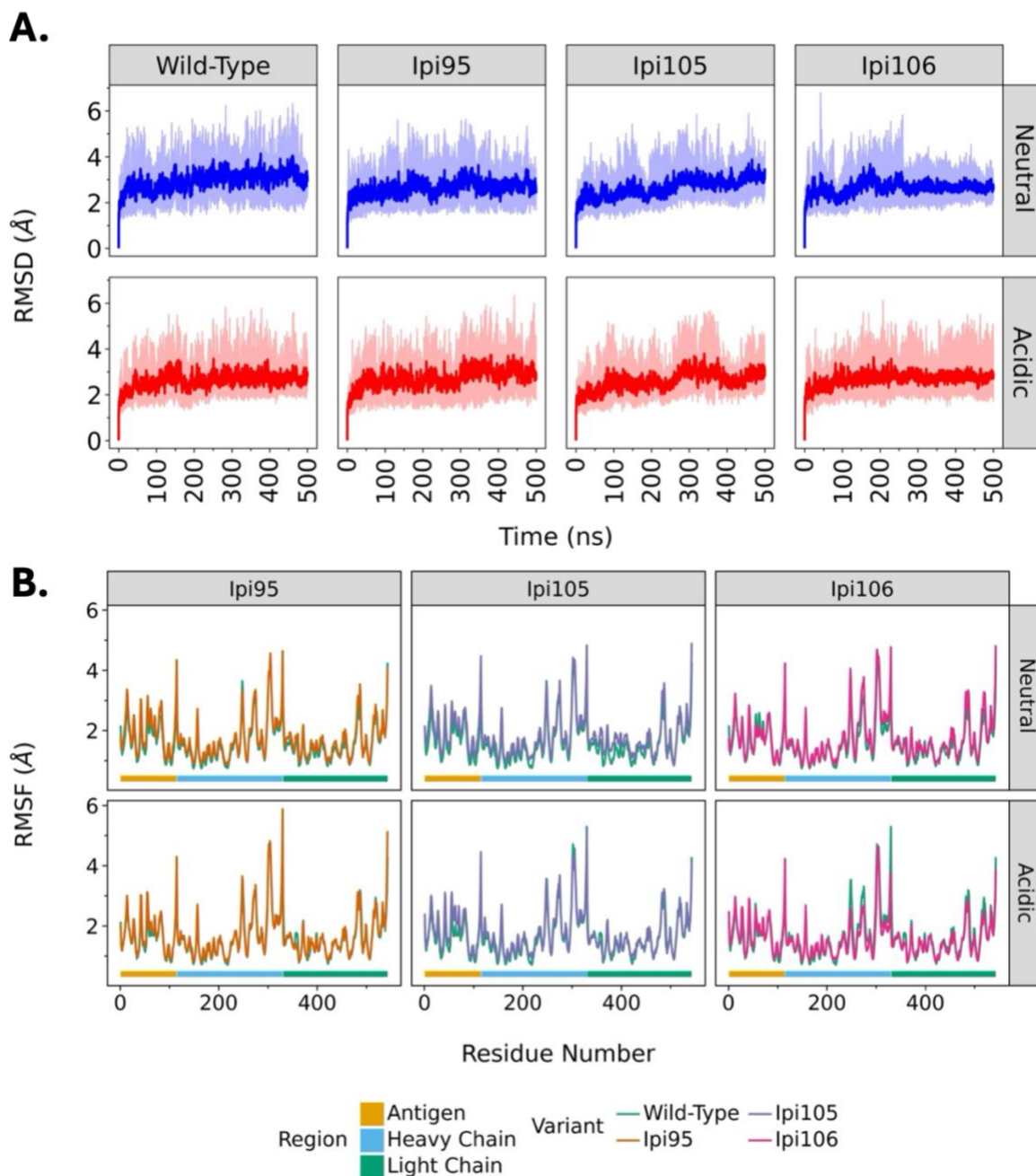


Table S3. Statistical analysis of MM/GBSA-based binding energy values to compare Ipilimumab–CTLA-4 complex binding in physiological and acidic conditions.

Saphiro-Wilk test for normality					
No	Variants	<i>p</i> -value > 0.05 = normal			
		Physiological		Acidic	
1	Wild-Type	0.0141		0.0752	
2	Ipi95	0.1154		0.0141	
3	Ipi105	0.0075		0.0392	
4	Ipi106	0.3702		0.5367	
Trimmed - Mean Permutation test for difference between physiological and acidic condition					
No	Variants	<i>p</i> -value		Significancy	
1	Wild-Type	0.4133		ns	
2	Ipi95	0.0028		**	
3	Ipi105	0.0082		**	
4	Ipi106	0.0056		**	
Cohen's d and Cliff's Delta test for practical significance					
No	Variants	Cohen's d		Cliff's Delta	
1	Wild-Type	0.5675	(Medium)	0.2096	(Small)
2	Ipi95	1.0721	(Large)	0.5200	(Large)
3	Ipi105	0.7212	(Medium)	0.3696	(Medium)
4	Ipi106	0.7243	(Medium)	0.3888	(Medium)

Figure S3. Distributions of radius of gyration (R_g) of the antigen–antibody interfaces calculated using CPPTRAJ for over five 500-ns MD replicas.⁵ The values of R_g reflect the compactness of binding in the physiological (blue) and acidic conditions (red). Graphs were generated using ggplot2 in JupyterLab.⁴

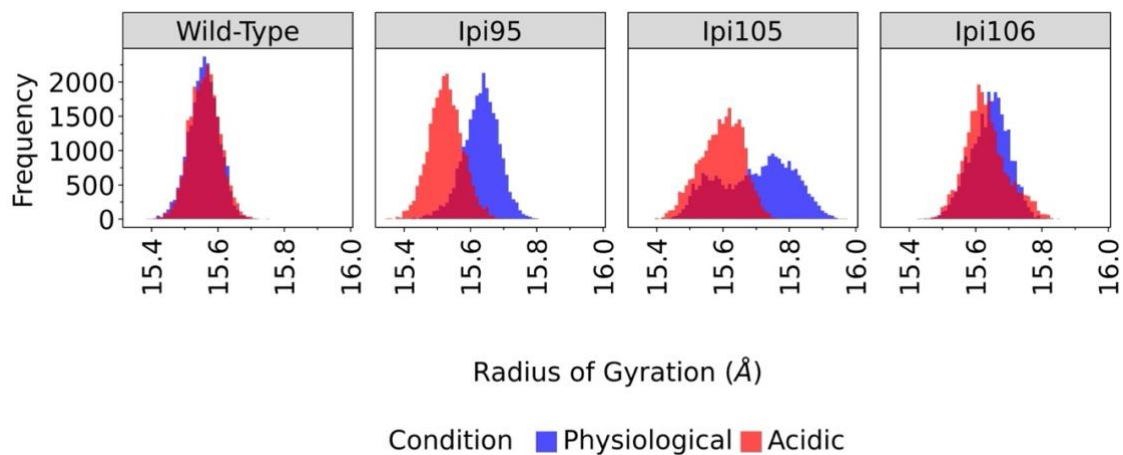


Table S4. Residue interaction network analyses of all Ipilimumab variants under the physiological and acidic conditions based on the trajectories of 500-ns MD simulations using RING4.0.⁷

Mutation	Amino Acid	Condition	RIN Analysis*				Results
			Wild-Type	Ipi95	Ipi105	Ipi106	
H – S31H	S31	Physiological	Green	Grey	Grey	Grey	No difference
		Acidic	Green	Grey	Grey	Grey	
	H31	Physiological	Grey	Blue	Blue	Blue	Better in Physiological
		Acidic	Grey	Green	Green	Yellow	
H – N56H	N56	Physiological	Blue	Grey	Grey	Grey	No difference
		Acidic	Blue	Grey	Grey	Grey	
	H56	Physiological	Grey	Blue	Grey	Grey	Better in Acidic
		Acidic	Grey	Blue	Green	Grey	
H – T99H	T99	Physiological	Yellow	Yellow	Yellow	Grey	Better in Acidic
		Acidic	Yellow	Green	Green	Grey	
	H99	Physiological	Grey	Grey	Grey	Blue	No difference
		Acidic	Grey	Grey	Grey	Blue	
L – S28E	S28	Physiological	Grey	Grey	Grey	Grey	No difference
		Acidic	Grey	Grey	Grey	Grey	
	E28	Physiological	Grey	Grey	Grey	Grey	No difference
		Acidic	Grey	Grey	Grey	Grey	
L – S31E/D	S31	Physiological	Blue	Grey	Grey	Grey	Better in Physiological
		Acidic	Grey	Grey	Grey	Grey	
	E31	Physiological	Grey	Grey	Grey	Grey	Better in Acidic
		Acidic	Grey	Grey	Blue	Grey	
	D31	Physiological	Grey	Blue	Grey	Grey	Better in Physiological
		Acidic	Grey	Grey	Grey	Grey	
L – Y33E	Y33	Physiological	Yellow	Grey	Grey	Grey	Better in Acidic
		Acidic	Blue	Grey	Grey	Grey	
	E33	Physiological	Grey	Blue	Blue	Blue	No difference

*Different colors represent the interaction type in each residue. Grey: blank cells; White: no interaction; Yellow: intermolecular interaction; Green: indirect interaction; Blue: direct interaction. This analysis categorizes residue types from the least to the most favorable interactions between each antigen-antibody pair.

Figure S4. Correlation between experimental and computational average binding energy values for all Ipilimumab variants based on MM/GBSA method ($\Delta G_{\text{MM/GBSA}}$), calculated using MMPBSA.py³ and visualized via linear regression in ggplot2.⁴ Blue (red) dots represent values under the physiological (acidic) conditions in partial (A) and full protonation state (B).

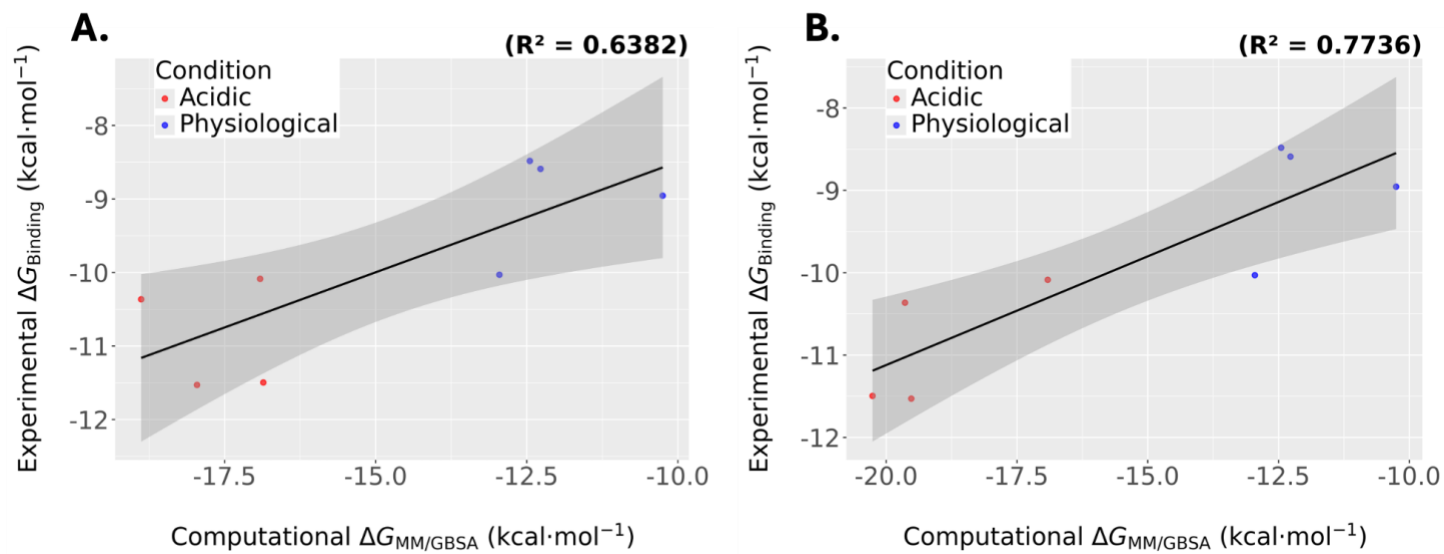


Figure S5. Representative-structure selection based on clustering analysis of five simulation replicas. Clustering was performed on the combined trajectories of five independent replicas for each variant under physiological and acidic conditions using *K*-means clustering in CPPTRAJ.⁵ The populations of the major clusters are shown for Wild-Type, Ipi95, Ipi105, and Ipi106. The most populated cluster, highlighted in each panel, was used to define the representative structure shown for each system. The plot was created with ggplot2 in JupyterLab.⁴

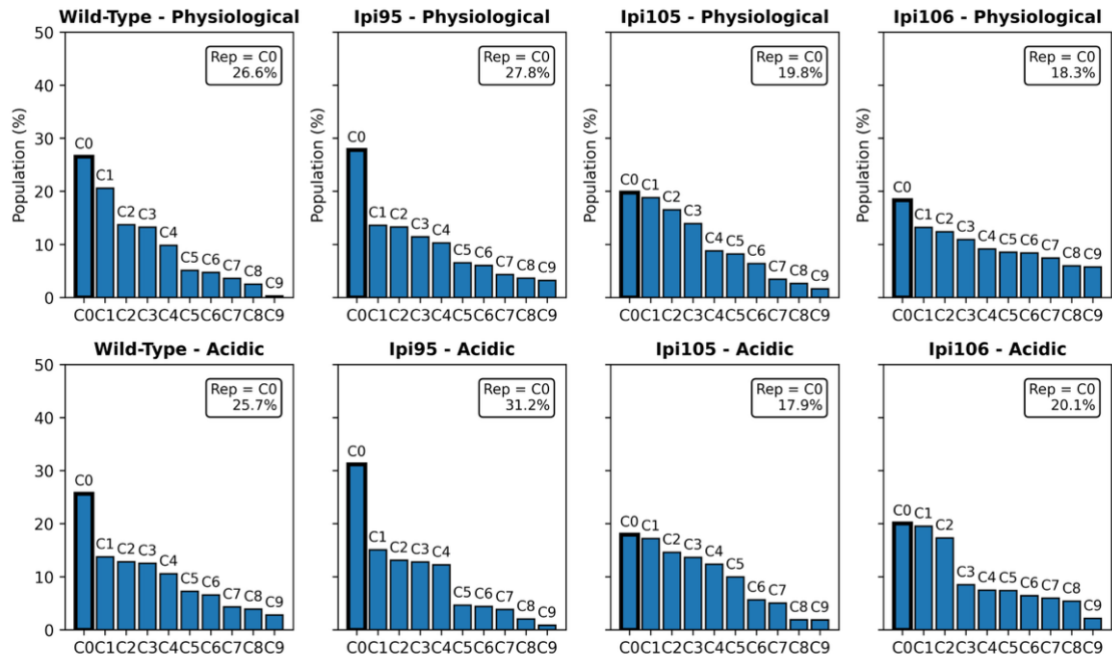


Figure S6. A set of representative conformations illustrating structural variability across the 500 ns trajectories for each variant. The *K*-means clustering was conducted using CPPTRAJ,⁵ and visualized using ChimeraX.⁶

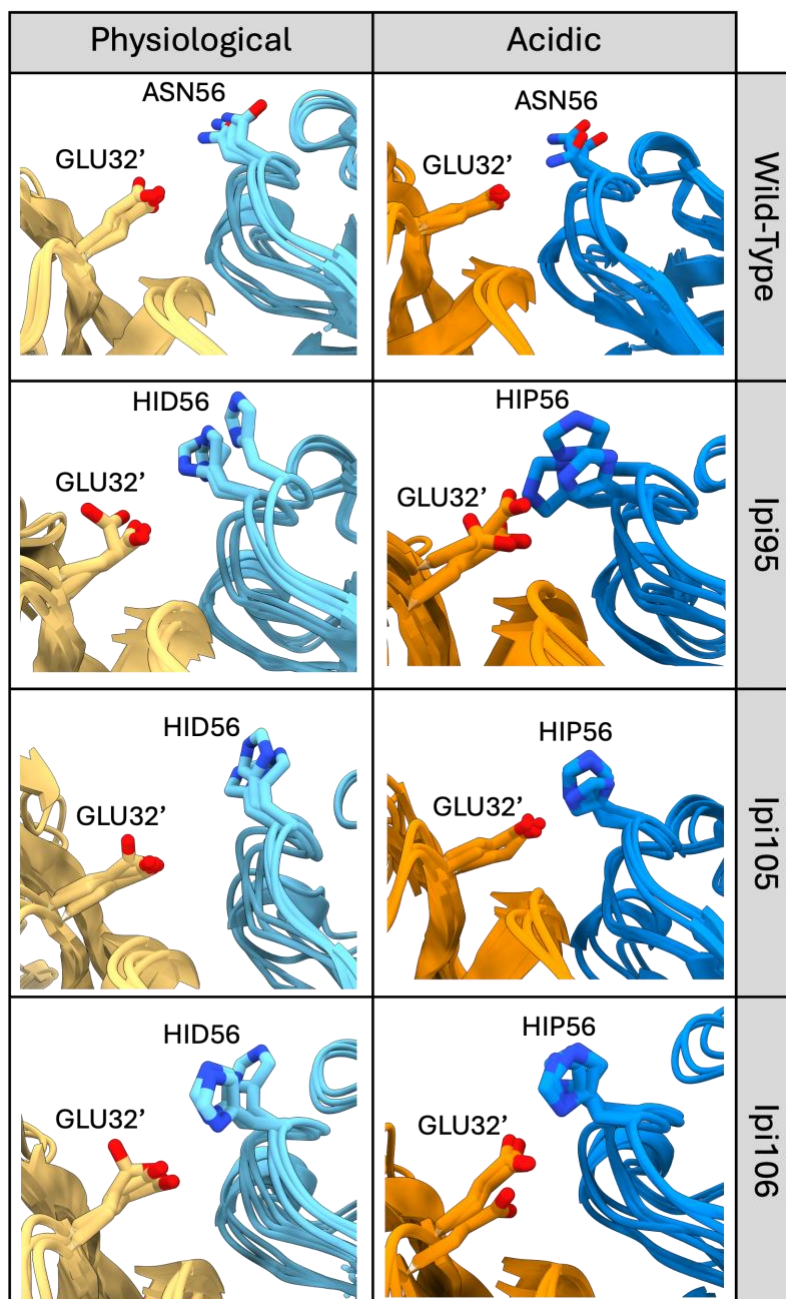
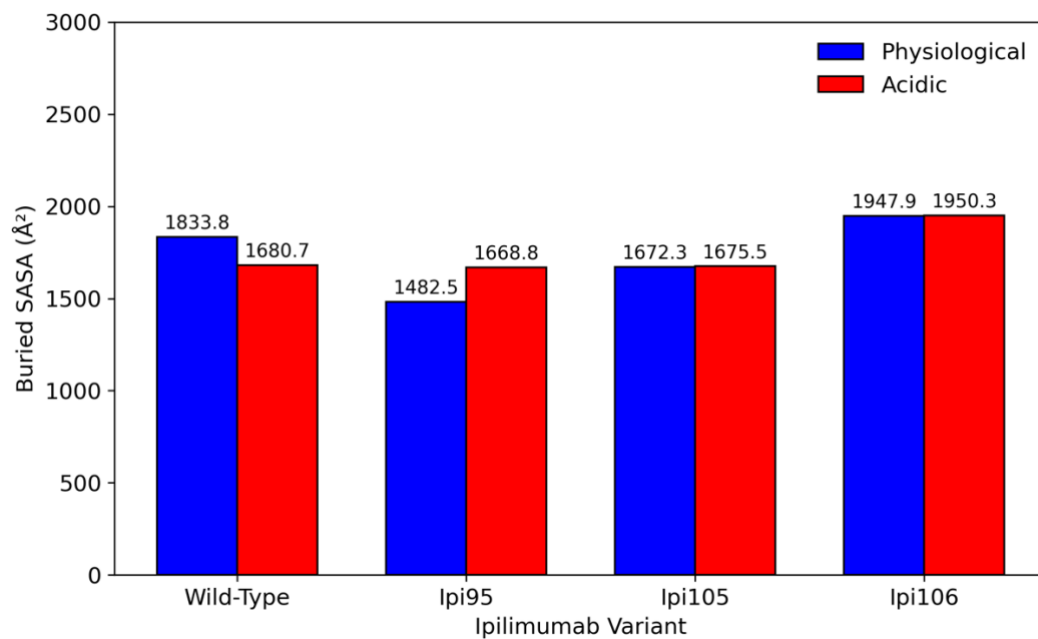


Figure S7. The buried SASA of each representative structure in all systems confirms the most prominent Ipilimumab variant (Ipi95) calculated as $SASA_{\text{antigen}} + SASA_{\text{antibody}} - SASA_{\text{complex}}$. The SASA analysis was conducted using CPPTRAJ.⁵ The plot was created with ggplot2 in JupyterLab.⁴



REFERENCES

- 1 T. J. Dolinsky, P. Czodrowski, H. Li, J. E. Nielsen, J. H. Jensen, G. Klebe and N. A. Baker, PDB2PQR: Expanding and upgrading automated preparation of biomolecular structures for molecular simulations, *Nucleic Acids Res.*, 2007, **35**, 522–525.
- 2 D. S. BIOVIA, Biovia Discovery Studio 2024, *Dassault Systèmes*, 2024.
- 3 B. R. Miller, T. D. McGee, J. M. Swails, N. Homeyer, H. Gohlke and A. E. Roitberg, MMPBSA.py: An efficient program for end-state free energy calculations, *J. Chem. Theory Comput.*, 2012, **8**, 3314–3321.
- 4 H. Wickham, *ggplot2: Elegant Graphics for Data Analysis*, Springer, New York, 1st edn., 2009.
- 5 D. R. Roe and T. E. Cheatham, PTRAJ and CPPTRAJ: Software for processing and analysis of molecular dynamics trajectory data, *J. Chem. Theory Comput.*, 2013, **9**, 3084–3095.
- 6 E. F. Pettersen, T. D. Goddard, C. C. Huang, E. C. Meng, G. S. Couch, T. I. Croll, J. H. Morris and T. E. Ferrin, UCSF ChimeraX: Structure visualization for researchers, educators, and developers, 2021, **30**, 70–82.
- 7 A. Del Conte, G. F. Camagni, D. Clementel, G. Minervini, A. M. Monzon, C. Ferrari, D. Piovesan and S. C. E. Tosatto, RING 4.0: Faster residue interaction networks with novel interaction types across over 35,000 different chemical structures, *Nucleic Acids Res.*, 2024, **52**, W306–W312.